High-Throughput Multi-Source Cooperation via Complex-Field Network Coding

Guobing Li, *Student Member, IEEE,* Alfonso Cano, *Member, IEEE,* Jesús Gómez-Vilardebó, *Member, IEEE,* Georgios B. Giannakis, *Fellow, IEEE,* and Ana I. Pérez-Neira, *Senior Member, IEEE*

***Abstract*—Physical-layer network coding over wireless networks can provide considerable throughput gains with respect to traditional cooperative relaying strategies at no loss of diversity gain. In this paper, a novel cooperation protocol is developed based on complex-field wireless network coding. Sources transmit efficiently information symbols linearly combined with symbols from other sources. Different from existing wireless network coding protocols, transmissions are not restricted to binary symbols, and do not have to be received simultaneously. In a network with N sources, the developed protocol can achieve throughput up to approximately $1/N$ symbols per source per channel use, as well as diversity of order N. To deal with decoding errors at sources, selective- and adaptive-forwarding protocols are also developed at no loss of diversity gain. Analytical results corroborated by simulated tests show considerable performance gains with respect to distributed space-time coding, and bit-level network coding protocols.**

***Index Terms*—Cooperative diversity, network coding, multi-source cooperation.**

I. Introduction

THANKS to the broadcast nature of wireless channels, capacity and diversity gains can be achieved through cooperation of distributed users [15], [16]. However, as the number of users grows, traditional cooperative schemes that relay redundant information incur throughput loss [18], [20], [5]. To increase throughput, wireless network coding (WNC) has been recently considered in wireless cooperative networks.

Manuscript received June 20, 2010; revised October 17 and December 24, 2010; accepted February 5, 2011. The associate editor coordinating the review of this paper and approving it for publication was H. Shin.

This work was supported by the NSF grants CCF-0830480, CCF-1016605, ECCS-0824007, and ECCS-1002180; the China Scholarship Council, Projects in Science and Technology of China (2009ZX03003-008-002); the NSFC under grants 60872028, 60902043 and 60902045; the Catalan Government under grants SGR2009-1046, SGR2009-0891; the Spanish Government under grant TEC2010-17816 and TEC2008-06327-C03-01; and the European project ICT-2007.1.1 NEWCOM++ 216715. Part of this work was presented at the Intl. Conf. on Acoustics, Speech and Signal Processing, Taipei, Taiwan, April 19-24, 2009, and the Wrkshp. on Signal Processing Advances in Wireless Communications, Marrakech, Marocco, June 20-23, 2010.

G. Li is with the School of Electronic and Information Engineering, Xi'an Jiaotong University, Xi'an, 710049, Shaanxi, PRC (e-mail: gbli@mail.xjtu.edu.cn). This work was performed during his visit at the University of Minnesota.

A. Cano and G. B. Giannakis are with the Department of Electrical and Computer Engineering, University of Minnesota, MN 55455, USA (e-mail: {alfonso, georgios}@umn.edu).

J. Gómez-Vilardebó and A. I. Pérez-Neira are with the Centre Tecnològic de Telecomunicacions de Catalunya, 08860 Castelldefels, Catalonia, Spain. A. I. Pérez-Neira is also with the Universitat Politècnica de Catalunya, 08034 Barcelona, Catalonia, Spain (e-mail: jesus.gomez@cttc.cat, ana.isabel.perez@upc.edu).

Digital Object Identifier 10.1109/TWC.2011.030911.101077

Network coding was originally developed for wireline networks [1], but was soon followed by corresponding developments for wireless networks [8], [13]. A number of WNC schemes assume that binary Galois Field GF(2) operations are effected "in the air" when multiple sources transmit packets that arrive simultaneously at the destination [21], [30]. In search of further rate improvements in multi-user scenarios, recent works have expanded the alphabet from GF(2) to GF(2^n) [14], [25], or, even to the complex field [21]. However, the network throughput is limited by this expansion and existing schemes are confined to two sources, or, still require simultaneous receptions.

Other than throughput, diversity order is another performance metric adopted for analysis of small networks with fading links. Critical to the diversity order achieved by WNC protocols is the processing performed at intermediate retransmissions [5], [21]. If relay nodes can afford analog processing and storage, diversity-enabling signal-amplification methods are derived in [2], [29]. Alternatively, packets can be decoded before retransmission. In this case, diversity can be achieved if only correctly decoded packets are forwarded, otherwise they are discarded [10], [23], [24]. However, relaying packets selectively eventually leads to the dismissal of entire packets even when the number of erroneously decoded bits within the packet is small, ultimately affecting the error performance. Decoding performance at the destination can be improved by forwarding error-prone packets, as in [28], although this requires the destination to know the error probability at all other links. Another approach entails power-adaptive transmissions, which are capable of achieving high diversity without knowing the error probability at intermediate steps [21].

The present paper develops a novel cooperation scheme using complex-field network coding (CFNC) for multi-source wireless networks. Sources transmit symbols (not necessarily binary) formed as a linear combination of new and previously-decoded symbols from other sources - an operation that can be viewed as a practical implementation of block-Markov coding [9]. Different source transmissions are channelized over time-orthogonal channels, thus avoiding interference. To deal with errors at intermediate nodes, two protocols are introduced: a) CFNC with selective forwarding (SF); and b) CFNC with link-adaptive forwarding (LAF). In CFNC-SF intermediate nodes re-transmit only correct information assuming bits were encoded using error-detecting (e.g., CRC) codes; whereas in CFNC-LAF re-transmitted symbols are weighted according to the intended link quality. In a network

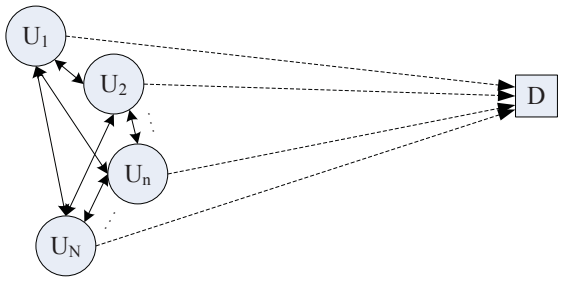

Fig. 1. N-source cooperation network.

with N cooperating sources, the throughput of this scheme is approximately $1/N$ symbols per source per channel use (spspcu), and the diversity is the maximum achievable (N). The novel protocol improves throughput of the state-of-the-art multi-source cooperative schemes ($1/(2N)$) [5], [20][1], and approaches that of non-cooperative orthogonal multiple-access schemes that do not exploit diversity. Compared to the opportunistic schemes in [3] and [11], CFNC-SF and CFNC-LAF guarantee identical (fixed) delay for all users, and thus deterministic (not average) throughput per source. Likewise, they do not require instantaneous feedback from the destination.

The rest of this paper is organized as follows. Section II presents the transmission scheme assuming error-free inter-source links. Section III deals with the selective- and adaptive-forwarding protocols. Their performance is analyzed in Section IV. Simulated tests are the subject of Section V, and Section VI concludes the paper.

Notation: Upper (lower) boldface letters are used for matrices (vectors); $[\cdot]_{ij}$ ($[\cdot]_i$) for the i,j-th (i-th) entry of a matrix (vector); $(\cdot)^T$ stands for the transposition of a matrix or vector; $\mathbf{I}_N$ denotes the $N \times N$ identity matrix; diag($\mathbf{x}$) is a diagonal matrix with $\mathbf{x}$ on its diagonal; $\odot$ the Hadamard product; $\| \cdot \|$ the Frobenius norm; $\mathcal{CN}(\mu, \sigma^2)$ a complex Gaussian distribution with mean μ and variance σ^2; and $Q(x) = \frac{1}{\sqrt{2\pi}} \int_x^\infty e^{-x^2/2} dx$ the Gaussian tail function.

II. Multi-Source Cooperation Protocol

Consider a set of N sources $\{U_n\}_{n=1}^N$ communicating with a common access point or destination D, as is shown in Fig. 1. Information bits of each source are modulated and carried over constellation symbols. Let $\mathbf{x}_n := [x_n(0), \ldots, x_n(K-1)]^T$ denote the sequence of K symbols drawn from a finite-size constellation set $\mathcal{A}_s$ at source U_n, $n = 1, \ldots, N$. Transmissions are arranged in $K+1$ phases including an initialization (Phase-0) and termination (Phase-K). The protocol is initialized by transmitting $s_n(0) = x_n(0)$, $\forall n$; see Table I. At subsequent phases, e.g., Phase-k, $k = 1, \ldots, K-1$, each source U_n has available the set of symbols $\{x_m(k)\}_{m=1, m\neq n}^N$ from all other sources. (This assumption is removed in Section III where inter-source detection errors will be incorporated.) Source U_n constructs a symbol $s_n(k)$ by linearly combining its k-th constellation symbol $x_n(k)$ with $\{x_m(k-1)\}_{m=1,m\neq n}^N$. The resulting symbol $s_n(k)$ is given by (see also Table I)

$$s_n(k) = \theta_{nn} x_n(k) + \sum_{\substack{m=1 \\ m\neq n}}^{N} \theta_{nm} x_m(k-1) \tag{1}$$

where coefficients $\theta_{n1}, \ldots, \theta_{nN}$ are designed so that, for any two vectors $\mathbf{x}, \tilde{\mathbf{x}} \in \mathcal{A}_s^N$

$$|\boldsymbol{\theta}_n^T(\mathbf{x} - \tilde{\mathbf{x}})| \neq 0, \forall n \tag{2}$$

where $\boldsymbol{\theta}_n := [\theta_{n1}, \ldots, \theta_{nN}]^T$. This condition guarantees that $s_n(k)$ in (1) is unique for every possible set of symbols $x_n(k)$ and $\{x_m(k-1)\}_{m=1,m\neq n}^N$. This so-called *identifiability condition* has been utilized in the context of co-located and distributed wireless fading systems [26], [21]. The set of vectors $\boldsymbol{\theta}_1, \ldots, \boldsymbol{\theta}_N$ that guarantees (2) is not unique, but can always be found for any N [26]. These coefficients are independent of the channel coefficients or the information to be sent. Hence, sources and the destination can have them pre-stored to prevent excess overhead.

Symbol $s_n(k)$ in (1) is transmitted from source U_n to D. Transmissions from different sources occur in separate time slots to avoid interference, distributed synchronization concerns, and the need for full-duplex operation. Since each source transmits one symbol, Phase-k entails N channel uses. Let $y_n(k)$ denote the signal received at D when U_n transmits $s_n(k)$, and $y_{mn}(k)$ the signal received at U_n when U_m transmits $s_m(k)$. Assuming flat fading links, these received symbols are given by

$$y_n(k) = h_n s_n(k) + w_n(k) \tag{3}$$

$$y_{mn}(k) = h_{mn} s_m(k) + w_{mn}(k) \tag{4}$$

where $h_n \sim \mathcal{CN}(0, \sigma_n^2)$ ($h_{mn} \sim \mathcal{CN}(0, \sigma_{mn}^2)$) is the Rayleigh fading coefficient corresponding to the U_m-to-D (U_m-to-U_n) link; $w_n(k)$ ($w_{mn}(k)$) is the noise term, normalized to be $\mathcal{CN}(0,1)$. With average transmitting power $\bar{\gamma}$, the instantaneous received signal-to-noise ratio (SNR) of each U_n-to-D (U_m-to-U_n) link is $\gamma_n := |h_n|^2 \bar{\gamma}$ ($\gamma_{mn} := |h_{mn}|^2 \bar{\gamma}$) with expected value $\bar{\gamma}_n = \sigma_n^2 \bar{\gamma}$ ($\bar{\gamma}_{mn} = \sigma_{mn}^2 \bar{\gamma}$). Throughout, the following operational condition will be adopted.

(AS1) Fading coefficients of all U_m-U_n links, namely h_{mn}, and U_n-D links, namely h_n, are known at receiving ends via training (pilot) symbols sent from the transmitting ends.

At the end of Phase-k, each source has received information-bearing symbols from all other sources. Source U_n uses $y_{mn}(k)$, received from U_m, to obtain an estimate $\hat{x}_m^{(n)}(k)$ of $x_m(k)$ based on the maximum likelihood (ML) criterion [cf. (4)]

$$\hat{x}_m^{(n)}(k) = \arg \min_{x \in \mathcal{A}_s} \left\| y_{mn}(k) - h_{mn}\Big(\theta_{mm} x + \sum_{\substack{p=1 \\ p\neq m}}^{N} \theta_{mp} x_p(k-1)\Big) \right\|^2 \tag{5}$$

where h_{mn} is assumed known at U_n [cf. (AS1)]. Since symbols $x_p(k-1)$ are known, the originally-transmitted symbol $x_m(k)$ is identifiable; i.e., in the absence of noise, the minimum of (5) is unique.

[1]Mappings in [5] and [20] also mix (over the complex field) information from different users, and in this sense they can also be viewed as performing a form of network coding.

TABLE I
TRANSMITTING SIGNALS OF THE MULTI-SOURCE COOPERATION PROTOCOL

	Phase 0	...	Phase k, $(k=1,2,...,K-1)$	...	Phase K
U_1	$x_1(0)$	...	$\theta_{11}x_1(k)+\sum_{m=2}^{N}\theta_{1m}\hat{x}_m^{(1)}(k-1)$	...	$\sum_{m=2}^{N}\theta_{1m}\hat{x}_m^{(1)}(K-1)$
...	...	...	...	...	...
U_n	$x_n(0)$	...	$\theta_{nn}x_n(k)+\sum_{m=1,m\neq n}^{N}\theta_{nm}\hat{x}_m^{(n)}(k-1)$	...	$\sum_{m=1,m\neq n}^{N}\theta_{nm}\hat{x}_m^{(n)}(K-1)$
...	...	...	...	...	...
U_N	$x_N(0)$	...	$\theta_{NN}x_N(k)+\sum_{m=1}^{N-1}\theta_{Nm}\hat{x}_m^{(N)}(k-1)$	...	$\sum_{m=1}^{N-1}\theta_{Nm}\hat{x}_m^{(N)}(K-1)$

If sources incur no detection errors, then $\hat{x}_m^{(n)}(k) = x_m(k)$, $\forall m,n,k$, and all sources know $\{x_n(k)\}_{n=1}^N$, the *new* information symbols sent during Phase-k. With $\{x_m(k)\}_{m=1,m\neq n}^N$ and $x_n(k+1)$ available, U_n proceeds to Phase-$(k+1)$ up until Phase-K, where $s_n(K)$ $\forall n$ is [cf. (1)]

$$s_n(K)=\sum_{\substack{m=1\\m\neq n}}^{N}\theta_{nm}x_m(K-1). \tag{6}$$

The purpose of sending $s_n(K)$ is to guarantee that the last-transmitted symbols are also "diversified" through the channels in the same way the previous symbols were.

A. Decoding at the destination

Having received signals $\mathbf{y}:=[\{\{y_n(k)\}_{n=1}^N\}_{k=0}^K]^T$, from all sources after all $K+1$ phases, and assuming knowledge of the U_n-D link $\forall n$, the ML detection rule at D to jointly detect the information symbols sent from all sources, compactly expressed as the set $\boldsymbol{x}:=\{\{x_n(k)\}_{n=1}^N\}_{k=0}^K$, is

$$\hat{\boldsymbol{x}}^{\mathrm{ML}}=\arg\min_{\boldsymbol{x}\in\mathcal{A}_s^{KN}}\left\{\sum_{n=1}^{N}\|y_n(0)-h_nx_n(0)\|^2+\sum_{k=1}^{K-1}\sum_{n=1}^{N}\left\|y_n(k)-h_n\left(\theta_{nn}x_n(k)+\sum_{\substack{m=1\\m\neq n}}^{N}\theta_{nm}x_m(k-1)\right)\right\|^2+\sum_{n=1}^{N}\left\|y_n(K)-h_n\sum_{\substack{m=1\\m\neq n}}^{N}\theta_{nm}x_m(K-1)\right\|^2\right\}. \tag{7}$$

If $\mathbf{h}:=[h_1,\ldots,h_N]^T$ denotes the vector collecting the channel coefficients of all sources with the destination, the detector in (7) can be written in matrix-vector form as

$$\hat{\boldsymbol{x}}^{\mathrm{ML}}=\arg\min_{\boldsymbol{x}\in\mathcal{A}_s^{NK}}\left\{\|\mathbf{y}-\boldsymbol{\Gamma}_x\mathbf{h}\|^2\right\} \tag{8}$$

where $\boldsymbol{\Gamma}_x$ is an $N(K+1)\times N$ matrix defined as

$$\boldsymbol{\Gamma}_x:=\begin{bmatrix}\mathbf{D}_x(0)\\(\boldsymbol{\Theta}\mathbf{D}_x(1)+\boldsymbol{\Theta}\mathbf{X}(0))\odot\mathbf{I}_N\\\vdots\\(\boldsymbol{\Theta}\mathbf{D}_x(k)+\boldsymbol{\Theta}\mathbf{X}(k-1))\odot\mathbf{I}_N\\\vdots\\(\boldsymbol{\Theta}\mathbf{D}_x(K-1)+\boldsymbol{\Theta}\mathbf{X}(K-2))\odot\mathbf{I}_N\\(\boldsymbol{\Theta}\mathbf{X}(K-1))\odot\mathbf{I}_N\end{bmatrix} \tag{9}$$

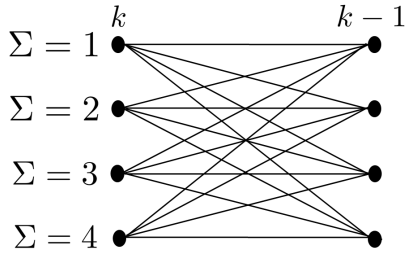

Fig. 2. Trellis diagram for $N=2$ and BPSK modulation ($|\mathcal{A}_s|^N=4$).

where $\mathbf{D}_x(k):=\mathrm{diag}(x_1(k),\ldots,x_N(k))$, $\boldsymbol{\Theta}:=[\boldsymbol{\theta}_1,\ldots,\boldsymbol{\theta}_N]^T$ and

$$\mathbf{X}(k):=\begin{bmatrix}0&x_1(k)&\cdots&x_1(k)\\x_2(k)&0&\cdots&x_2(k)\\\vdots&\vdots&\ddots&\vdots\\x_N(k)&x_N(k)&\cdots&0\end{bmatrix}. \tag{10}$$

The complexity of (8) is exponential in the number of sources (N), the block length (K), and the logarithm of the constellation size ($|\mathcal{A}_s|$). In principle, (8) could be written in a form readily suggesting applicability of linear detectors. However, these detectors cannot collect the full diversity. Complexity can be reduced without loss in error performance if one takes into account that symbols overlap across phases, thus introducing memory per transmitted block. This allows application of Viterbi's algorithm for ML demodulation [19].

Fig. 2 represents one stage of the associated trellis diagram. Every path in the complete trellis indicates a possible sequence of blocks $\mathbf{D}_x(0),\ldots,\mathbf{D}_x(K-1)$. The diagram has $|\mathcal{A}_s|^N$ bold dots, which indicate the possible states Σ, corresponding to the different values $\mathbf{D}_x(k)$ can take. Each line in Fig. 2 is associated with a new block $\mathbf{D}_x(k)$ (next state), a previous block $\mathbf{D}_x(k-1)$ (previous state), and a received block $\mathbf{y}(k):=[y_1(k),\ldots,y_N(k)]^T$. The branch metric between states $k-1$ and k is

$$\|\mathbf{y}(k)-([\boldsymbol{\Theta}\mathbf{D}_x(k)+\boldsymbol{\Theta}\mathbf{X}(k-1)]\odot\mathbf{I}_N)\mathbf{h}\|^2. \tag{11}$$

For the initial and final state transitions, the metrics are $\|\mathbf{y}(0)-\mathbf{D}_x(0)\mathbf{h}\|^2$ and $\|\mathbf{y}(K)-([\boldsymbol{\Theta}\mathbf{X}(K-1)]\odot\mathbf{I}_N)\mathbf{h}\|^2$, respectively. From these branch metrics, the path metric can be computed according to the Viterbi algorithm. The decoded sequence of blocks $\mathbf{D}_x(0),\ldots,\mathbf{D}_x(K-1)$ forming $\hat{\boldsymbol{x}}^{\mathrm{ML}}$ in (8) will be the one with the lowest path metric.

B. Performance analysis

The proposed protocol requires $(K+1)N$ channel uses to transmit K symbols per source. Defining the throughput η as

the number of transmitted information symbols per source per channel use (spspcu), it holds that

$$\eta = \frac{K}{(K+1)N} \text{ spspcu.} \tag{12}$$

For large K, η approaches $1/N$, which is the throughput of a non-cooperative scheme transmitting over orthogonal channels.

Another relevant performance metric is the pairwise error probability (PEP), denoted by $\Pr(\boldsymbol{x} \to \tilde{\boldsymbol{x}}|\mathbf{h}, \mathbf{h}^{(s)})$, and defined as the probability of decoding a set of symbols $\tilde{\boldsymbol{x}} \in \mathcal{A}_s^{KN}$ different from the transmitted $\boldsymbol{x}$, averaged w.r.t. the inter-source channel coefficients $\mathbf{h}^{(s)} := [h_{11}, \ldots, h_{1N}, \ldots, h_{NN}]^T$ between sources, and $\mathbf{h}$. The diversity order d can be correspondingly defined as the slope of the logarithm of the average pairwise error probability at the destination; that is,

$$d := \min_{\boldsymbol{x}, \tilde{\boldsymbol{x}} \neq \boldsymbol{x}} \left\{ -\lim_{\bar{\gamma} \to \infty} \frac{\log \mathbb{E}_{\mathbf{h}, \mathbf{h}^{(s)}} \left[\Pr(\boldsymbol{x} \to \tilde{\boldsymbol{x}}|\mathbf{h}, \mathbf{h}^{(s)}) \right]}{\log \bar{\gamma}} \right\}. \tag{13}$$

Provided that sources commit no decoding errors, the PEP does not depend on $\mathbf{h}^{(s)}$ and corresponds to that of a co-located multi-antenna system [5]. Using the Chernoff bound, it can be bounded as

$$\Pr(\boldsymbol{x} \to \tilde{\boldsymbol{x}}|\mathbf{h}) \leq \kappa_1 \exp\left(-\kappa_2 \|(\mathbf{\Gamma}_x - \mathbf{\Gamma}_{\tilde{x}})\mathbf{h}\|^2\right) \tag{14}$$

where κ_1 and κ_2 are positive constants, and $\mathbf{\Gamma}_{\tilde{x}}$ is defined as $\mathbf{\Gamma}_x$ after replacing $x_n(k)$ by $\tilde{x}_n(k)$ in (9) and (10), $\forall n, k$. Taking the expected value of (14) w.r.t. $\mathbf{h}$ yields the average PEP as

$$\mathbb{E}_{\mathbf{h}}[\Pr(\boldsymbol{x} \to \tilde{\boldsymbol{x}}|\mathbf{h})] \leq \left(\bar{\beta}\bar{\gamma}\right)^{-\text{rank}(\mathbf{\Gamma}_x - \mathbf{\Gamma}_{\tilde{x}})} \tag{15}$$

for some finite constant $\bar{\beta}$. Substituting (15) into (13), the diversity order d is found dependent on the rank of $\mathbf{\Gamma}_x - \mathbf{\Gamma}_{\tilde{x}}$, as stated in the following proposition.

Proposition 1. *(No inter-source errors) The diversity order achieved by the cooperative scheme as described in Table I using the detector* (8)*, and assuming error-free inter-source links, is*

$$d = \textit{rank}(\mathbf{\Gamma}_x - \mathbf{\Gamma}_{\tilde{x}}) = N. \tag{16}$$

Proof: See Appendix A. ∎

Thus, in the error-free case, this protocol achieves the maximum possible diversity order N, equal to the number of sources. Because the number of blocks and bits per block transmitted by each source is the same, all sources achieve the same diversity order. Appendix A shows that the identifiability criterion in (2) is instrumental to prove Proposition 1. Without this condition, the ML decoder in (8) would still be valid, but diversity may not be enabled; i.e., matrix $\mathbf{\Theta}$ acts as a precoding module. Indeed, if $\mathbf{\Theta}$ is, e.g., the all-ones matrix (normalized by $\sqrt{N}$), it is always possible to find specific blocks $\boldsymbol{x} \neq \tilde{\boldsymbol{x}}$ so that the rank of $(\mathbf{\Gamma}_x - \mathbf{\Gamma}_{\tilde{x}})$ is less than N. Finally, notice also that the diversity in (16) is independent of $\sigma_1^2, \ldots, \sigma_N^2$ ($\sigma_{11}^2, \ldots, \sigma_{NN}^2$), the channel statistics of source-destination (inter-source) links.

Remark 1. (*Comparison with distributed space-time and network coding*) Compared to the state-of-the-art multi-source cooperative schemes [18], [20], [5], this novel protocol achieves the same diversity performance at no loss of throughput, approaching that of non-cooperative orthogonal multiple-access schemes that do not exploit diversity ($1/N$ spspcu). Compared to [24], the present scheme is not restricted to bit-level operations. Moreover, it will allow the development of adaptive schemes whereby erroneous symbols can still be forwarded. This is precisely one of the objectives in the ensuing section.

III. Selective and Link-Adaptive Forwarding Protocols

Consider now the more realistic scenario where the m-th decoded symbol $\hat{x}_m^{(n)}(k)$ at U_n per Phase-k, can differ from $x_m(k)$, $\forall m \neq n$. The following forwarding strategies will be explored.

A. Selective forwarding protocol

In the SF protocols of e.g., [20] and [4], symbol $\hat{x}_m^{(n)}(k)$ is only forwarded if it is equal to $x_m(k)$, otherwise it is discarded. In practice, relaying selectively information in a throughput-efficient manner is performed on a per-packet basis; i.e., source U_n per Phase-k transmits a block of symbols instead of $s_n(k)$ alone. Notwithstanding, since packet transmissions do not affect throughput or diversity claims, and for simplicity of exposition, symbol-by-symbol operation will be described here. Error detection codes can be used at the transmitter to guarantee that the receiver can detect errors within the packet. In the analysis henceforth, the following assumption is made.

(AS2) The error-detection code is perfect, and incurs no loss in spectral efficiency.

With $\hat{x}_m^{(n)}(k)$ as in (5), define $\mathcal{D}_n(k) := \{m \mid \hat{x}_m^{(n)}(k) = x_m(k), m \in \{1, \ldots, N\}, m \neq n\}$ as the set of symbols source U_n correctly detected at the k-th slot, excluding index n. Source U_n will construct $s_n(k)$ by jointly encoding the correctly-received symbols indexed by $\mathcal{D}_n(k-1)$ along with its own *next* information symbol $x_n(k)$. In the CFNC-SF protocol, symbol $s_n(k)$ at source U_n is now constructed as [c.f. (1)]

$$s_n(k) = \theta_{nn} x_n(k) + \sum_{m \in \mathcal{D}_n(k-1)} \theta_{nm} x_m(k-1). \tag{17}$$

Note that $s_n(k)$ will always be non-zero even if $\mathcal{D}_n(k-1)$ is empty. Symbol $s_n(k)$ is transmitted to all other sources and to the destination as in (3) and (4). It is also assumed that:

(AS3) Source U_n informs other sources and the destination about the set of correctly-decoded symbols $\mathcal{D}_n(k-1)$ used to encode $s_n(k)$.

Since $\mathcal{D}_n(k-1)$ can take 2^{N-1} possible values, $N-1$ extra bits will be used for this purpose. This overhead information is fixed regardless of the packet size used for transmission.

Since the transmitted symbols have been modified, so has to be the detection rule in (5). Let $\mathcal{C}_{mn}(k) := \mathcal{D}_m(k) \cap (\mathcal{D}_n(k) \cup \{n\})$ denote the set of symbol indices correctly

decoded by both U_n and U_m. Likewise, define $\mathcal{F}_{mn}(k) := \mathcal{D}_m(k) \cap \overline{(\mathcal{D}_n(k) \cup \{n\})}$ as the set of symbols correctly decoded by U_m but erroneously decoded by U_n, and thus are unknown to U_n. Using these definitions, the following decoding rule is implemented at each source node [cf. (5)]

$$\hat{\mathbf{x}}_m^{(n)}(k) = \arg \min_{\bar{\mathbf{x}} \in \mathcal{A}_s^{|\mathcal{F}_{mn}(k-1)|+1}} \Big\| y_{mn}(k) - h_{mn}\Big(\theta_{mm}\bar{x}_m + \sum_{p \in \mathcal{F}_{mn}(k-1)} \theta_{mp}\bar{x}_p + \sum_{q \in \mathcal{C}_{mn}(k-1)} \theta_{mq} x_q(k-1)\Big)\Big\|^2 \quad (18)$$

where $\bar{x}_p := [\bar{\mathbf{x}}]_p$. If $\mathcal{F}_{mn}(k-1) = \emptyset$ and $\mathcal{C}_{mn}(k-1) = \{q | q = 1, \ldots, N; q \neq m\}$, the rule in (18) reduced to the one in (5), which assumes no decoding errors at both U_n and U_m in Phase-$(k-1)$. If however $\mathcal{F}_{mn}(k-1) \neq \emptyset$, source U_n decodes the symbol of interest $x_m(k)$ plus other symbols it did not decode during Phase-$(k-1)$ indexed by $\mathcal{F}_{mn}(k-1)$. If source U_n treated $\bar{x}_p$, $p \in \mathcal{F}_{mn}(k-1)$, as noise, the detector in (18) would not be ML. This is the reason why the decoding rule in (18) is defined for all $\bar{\mathbf{x}} \in \mathcal{A}_s^{|\mathcal{F}_{mn}(k-1)|+1}$. Notice also that the identifiability condition in (2) guarantees that $\bar{\mathbf{x}}$ is uniquely identifiable, regardless of the size of $\mathcal{F}_{mn}(k-1)$. Finally, having decoded $\hat{\mathbf{x}}_m^{(n)}(k)$ in (18), U_m can extract $\hat{x}_m^{(n)}(k)$ from $\hat{\mathbf{x}}_m^{(n)}(k)$, update $\mathcal{D}_n(k)$, and proceed to Phase-$(k+1)$.

At the destination, the ML detection rule that jointly detects the symbols sent from all sources is now given by [cf. (7)]

$$\hat{\boldsymbol{x}}^{ML} = \arg \min_{\boldsymbol{x} \in \mathcal{A}_s^{KN}} \Bigg\{ \sum_{n=1}^{N} \|y_n(0) - h_n x_n(0)\|^2 + \sum_{k=1}^{K-1} \sum_{n=1}^{N} \Big\| y_n(k) - h_n\Big(\theta_{nn}x_n(k) + \sum_{m \in \mathcal{D}_n(k-1)} \theta_{nm} x_m(k-1)\Big)\Big\|^2 + \sum_{n=1}^{N} \Big\| y_n(K) - h_n \sum_{m \in \mathcal{D}_n(K-1)} \theta_{nm} x_m(K-1)\Big\|^2 \Bigg\}. \quad (19)$$

With the super-set $\mathcal{D} := \{\{\mathcal{D}_n(k)\}_{n=1}^N\}_{k=0}^{K-1}$, the ML detector in (19) can be compactly written as

$$\hat{\boldsymbol{x}} = \arg \min_{\boldsymbol{x} \in \mathcal{A}_s^{NK}} \big\{ \|\mathbf{y} - \boldsymbol{\Gamma}_x(\mathcal{D})\mathbf{h}\|^2 \big\} \quad (20)$$

where $\boldsymbol{\Gamma}_x(\mathcal{D})$ is defined as in (9)-(10), after setting $[\mathbf{X}(k)]_{m,n} = 0$ for $m \notin \mathcal{D}_n(k)$. The Viterbi decoder as described in Section (II-A) can still be employed, now with a different path metric dependent on $\mathcal{D}_n(k)$.

B. Link-adaptive forwarding protocol

Dismissing erroneous symbols (packets) $\hat{x}_m^{(n)}$ when constructing $s_n(k)$ in (17) eventually leads to coding gain loss, since a CRC failure due to a single bit error implies dismissal of an entire packet. This section develops an alternative scheme in which erroneous symbols can still be included, after weighting them according to their reliability. In the CFNC-LAF protocol, source U_n constructs symbol $s_n(k)$ as [cf. (1) and (17)]:

$$s_n(k) = \theta_{nn}x_n(k) + \sqrt{\alpha_n} \sum_{\substack{m=1 \\ m \neq n}}^{N} \theta_{nm} \hat{x}_m^{(n)}(k-1) \quad (21)$$

where the scalar α_n in (21) is a link-adaptive forwarding coefficient defined as

$$\alpha_n := \beta \min\left\{ \min_{m \neq n} \frac{\gamma_{mn}}{\bar{\gamma}_n}, 1 \right\} \quad (22)$$

and β is a positive upper-bound on α_n, i.e., $\alpha_n \leq \beta$, $\forall n = 1, 2, ..., N$. The role of the LAF coefficient α_n is to weight (error-prone) estimated symbols [5], [7]. If $\{\gamma_{mn}\}_{m=1,m\neq n}^N$ exceed the average $\bar{\gamma}_n$, then α_n will be one; otherwise, α_n will be less than one, reducing the interference level of those symbols. To construct α_n, source U_n uses $\{\gamma_{mn}\}_{m=1,m\neq n}^N$ which is known through h_{mn} and $\bar{\gamma}_n$. This requires assuming the following.

(AS2') Source U_n knows its average channel to the destination $\bar{\gamma}_n$ via feedback.

The average channel to the destination $\bar{\gamma}_n$ varies slowly and thus can be fed back through a low-rate channel. Symbols $s_n(k)$ as in (21) are transmitted to the other sources and destination. In order to decode these symbols the next assumption is needed.

(AS3') Via training, source U_n knows $h_{mn}\sqrt{\alpha_m}$ and the destination knows $h_n\sqrt{\alpha_n}$. Fading coefficients h_n are not needed at the sources, which means that instantaneous feedback from the destination is not required.

Acquiring $h_{mn}\sqrt{\alpha_m}$ ($h_n\sqrt{\alpha_n}$) via training is similar to acquiring h_{mn} (h_n) as in (AS1) but now only with a pilot scaled by $\sqrt{\alpha_n}$; see also [22]. Consequently, the training overhead per link doubles with respect to CFNC-SF. Using this assumption, source U_n now employs the following decoder [cf. (5) and (18)]

$$\hat{x}_m^{(n)}(k) = \arg \min_{x \in \mathcal{A}_s} \Big\{ \Big\| y_{mn}(k) - h_{mn}\Big(\theta_{mm}x + \sqrt{\alpha_m} \sum_{\substack{p=1 \\ p \neq m}}^{N} \theta_{mp} \hat{x}_p^{(n)}(k-1)\Big)\Big\|^2 \Big\}. \quad (23)$$

Notice that the (error-prone) previously-decoded symbols $\hat{x}_p^{(n)}(k-1)$ are used in (23). The ML rule at the destination is likewise given by

$$\hat{\boldsymbol{x}} = \arg \min_{\boldsymbol{x} \in \mathcal{A}_s^{NK}} \big\{ \|\mathbf{y} - \boldsymbol{\Gamma}_{x,\alpha}\mathbf{h}\|^2 \big\} \quad (24)$$

where $\boldsymbol{\Gamma}_{x,\alpha}$ is [cf. (9)]

$$\boldsymbol{\Gamma}_{x,\alpha} := \begin{bmatrix} \mathbf{D}_x(0) \\ (\boldsymbol{\Theta}\mathbf{D}_x(1) + \mathbf{D}_\alpha\boldsymbol{\Theta}\mathbf{X}(0)) \odot \mathbf{I}_N \\ \vdots \\ (\boldsymbol{\Theta}\mathbf{D}_x(k) + \mathbf{D}_\alpha\boldsymbol{\Theta}\mathbf{X}(k-1)) \odot \mathbf{I}_N \\ \vdots \\ (\boldsymbol{\Theta}\mathbf{D}_x(K-1) + \mathbf{D}_\alpha\boldsymbol{\Theta}\mathbf{X}(K-2)) \odot \mathbf{I}_N \\ (\mathbf{D}_\alpha\boldsymbol{\Theta}\mathbf{X}(K-1)) \odot \mathbf{I}_N \end{bmatrix} \quad (25)$$

with $\mathbf{D}_\alpha := \text{diag}([\alpha_1, \ldots, \alpha_N])$.

Remark 2. (*CFNC-SF vs. CFNC-LAF*) Compared to CFNC-SF, the CFNC-LAF protocol in this section does not require to inform other sources and the destination about symbol error outages, thus reducing the extra overhead per packet. Instead,

the CFNC-LAF protocol requires sources and the destination to know, respectively, $h_{mn}\sqrt{\alpha_m}$ and $h_n\sqrt{\alpha_n}$ through training as well as $\bar{\gamma}_m$ through feedback. However, neither CFNC-SF nor CFNC-LAF requires instantaneous feedback of the fading coefficients h_n from the destination as assumed available by opportunistic approaches, such as [3], [11]. Also, both CFNC-SF and CFNC-LAF guarantee deterministic (as opposed to average) throughput per user. The next section will also show that they achieve full diversity.

IV. Performance bounds for CFNC-SF and CFNC-LAF

When inter-source errors are present, the PEP evaluation proceeds in two steps. First, the probability of having a particular set of decoded symbols $\hat{\boldsymbol{x}} := \{\{\hat{x}_m^{(n)}(k)\}_{n,m=1,m\neq n}^{N}\}_{k=0}^{K-1}$ is found. Second, the PEP at the destination given this set of decoded symbols (which is termed error-conditional PEP), is obtained. The latter is found by marginalizing over all possible estimated symbols $\hat{\boldsymbol{x}}$

$$\Pr(\boldsymbol{x}\to\tilde{\boldsymbol{x}}|\mathbf{h},\mathbf{h}^{(s)})=\sum_{\forall\hat{\boldsymbol{x}}}\Pr(\boldsymbol{x}\to\tilde{\boldsymbol{x}}|\mathbf{h},\mathbf{h}^{(s)},\hat{\boldsymbol{x}})\Pr(\hat{\boldsymbol{x}}|\mathbf{h}^{(s)}) \quad (26)$$

where $\Pr(\boldsymbol{x}\to\tilde{\boldsymbol{x}}|\mathbf{h},\mathbf{h}^{(s)},\hat{\boldsymbol{x}})$ is the PEP at the destination conditioned on a set $\hat{\boldsymbol{x}}$ of forwarded symbols, and $\Pr(\hat{\boldsymbol{x}}|\mathbf{h}^{(s)})$ is the probability of having such a set $\hat{\boldsymbol{x}}$ conditioned on $\mathbf{h}^{(s)}$.

A. CFNC-SF protocol

In this case, the decoder at the destination is independent of $\mathbf{h}^{(s)}$ [cf. (19)]. Thus, $\Pr(\boldsymbol{x}\to\tilde{\boldsymbol{x}}|\mathbf{h},\mathbf{h}^{(s)},\hat{\boldsymbol{x}})=\Pr(\boldsymbol{x}\to\tilde{\boldsymbol{x}}|\mathbf{h},\hat{\boldsymbol{x}})$, and the expected value of (26) can be split into the product of two terms

$$\begin{aligned}&\mathbb{E}_{\mathbf{h},\mathbf{h}^{(s)}}\left[\Pr(\boldsymbol{x}\to\tilde{\boldsymbol{x}}|\mathbf{h},\mathbf{h}^{(s)})\right]\\&\quad=\sum_{\forall\hat{\boldsymbol{x}}}\mathbb{E}_{\mathbf{h}}\left[\Pr(\boldsymbol{x}\to\tilde{\boldsymbol{x}}|\mathbf{h},\hat{\boldsymbol{x}})\right]\mathbb{E}_{\mathbf{h}^{(s)}}\left[\Pr(\hat{\boldsymbol{x}}|\mathbf{h}^{(s)})\right].\end{aligned} \quad (27)$$

Both factors on the right-hand side (r.h.s.) of (27) can be evaluated separately for a given (fixed) estimated set $\hat{\boldsymbol{x}}$. The second term on the r.h.s. of (27) can be obtained by first finding the conditional probability that source U_m detects $\hat{x}_n^{(m)}(k)\neq x_n(k)$. Using the Chernoff bound it can be bounded as $\Pr(x_n(k)\to\hat{x}_n^{(m)}(k)|\mathbf{h}^{(s)})\leq\exp\left(-\kappa_{mn}(k)|h_{mn}|^2\right)$ for some finite coefficient $\kappa_{mn}(k)$. Due to conditional independence, the conditional probability of detecting the entire set $\hat{\boldsymbol{x}}$ is thus

$$\Pr(\hat{\boldsymbol{x}}|\mathbf{h}^{(s)})\leq\exp\left(-\sum_{k=0}^{K-1}\sum_{n=1}^{N}\sum_{m\in\mathcal{E}_n(k)}\kappa_{mn}(k)|h_{mn}|^2\right) \quad (28)$$

where $\mathcal{E}_n(k)$ is the set of sources that failed to detect $x_n(k)$; i.e.,

$$\mathcal{E}_n(k):=\{m|n\notin\mathcal{D}_m(k),m=1,\ldots,N,m\neq n\} \quad (29)$$

with $\mathcal{D}_m(k)$ defined as in Section III-A. Note that for every estimated set $\hat{\boldsymbol{x}}$ there is a corresponding error set $\{\{\mathcal{E}_n(k)\}_{n=1}^{N}\}_{k=0}^{K-1}$. The expected value of (28) can be bounded by

$$\mathbb{E}_{\mathbf{h}^{(s)}}\left[\Pr(\hat{\boldsymbol{x}}|\mathbf{h}^{(s)})\right]\leq(\beta'\bar{\gamma})^{-\left|\cup_{n=1}^{N}\cup_{k=0}^{K-1}\mathcal{E}_n(k)\right|}=(\beta'\bar{\gamma})^{-|\mathcal{E}|} \quad (30)$$

where $\mathcal{E}:=\cup_{n=1}^{N}\cup_{k=0}^{K-1}\mathcal{E}_n(k)$, and the inequality holds at high SNR for some constant β'.

Back to (27), the first term on the r.h.s. is instead given by

$$\Pr(\boldsymbol{x}\to\tilde{\boldsymbol{x}}|\mathbf{h},\hat{\boldsymbol{x}})\leq\exp\left(-\kappa'\left\|(\boldsymbol{\Gamma}_x(\mathcal{D})-\boldsymbol{\Gamma}_{\tilde{x}}(\mathcal{D}))\mathbf{h}\right\|^2\right) \quad (31)$$

where $\boldsymbol{\Gamma}_{\tilde{x}}(\mathcal{D})$ is constructed as $\boldsymbol{\Gamma}_x(\mathcal{D})$ in (20), after replacing $x_n(k)$ by $\tilde{x}_n(k)$. The expected value of $\Pr(\boldsymbol{x}\to\tilde{\boldsymbol{x}}|\mathbf{h},\hat{\boldsymbol{x}})$ can be bounded as

$$\mathbb{E}_{\mathbf{h}^{(s)}}\left[\Pr(\boldsymbol{x}\to\tilde{\boldsymbol{x}}|\mathbf{h},\hat{\boldsymbol{x}})\right]\leq(\beta''\bar{\gamma})^{-\text{rank}(\boldsymbol{\Gamma}_x(\mathcal{D})-\boldsymbol{\Gamma}_{\tilde{x}}(\mathcal{D}))} \quad (32)$$

for some finite constant β''. Combining bounds (30) and (32), a bound on (27) can be established to access the diversity order of this scheme. The following proposition describes the final result.

Proposition 2. *(Diversity order of the CFNC-SF protocol) Consider the coefficients θ_{nm} $\forall n,m=1,\ldots,N$ selected to satisfy* (2)*. The diversity order as defined in* (13) *of the CFNC-SF protocol is*

$$d:=\min_{\boldsymbol{x},\tilde{\boldsymbol{x}}\neq\boldsymbol{x}}\left\{\text{rank}(\boldsymbol{\Gamma}_x(\mathcal{D})-\boldsymbol{\Gamma}_{\tilde{x}}(\mathcal{D}))+|\mathcal{E}|,N\right\}=N. \quad (33)$$

Proof: See Appendix B. ∎

Thus, the diversity order is independent of the intermediate set of estimated symbols $\hat{\boldsymbol{x}}$, and is equal to the number of sources N.

B. CFNC-LAF protocol

In the CFNC-LAF protocol, the decoder at the destination [cf. (24)] depends on the adaptive coefficients $\boldsymbol{\alpha}:=[\alpha_1,\ldots,\alpha_N]^T$, which in turn depend on the source-to-source channels $\mathbf{h}^{(s)}$ [cf. (22)]. Consequently, the average PEP in (27) cannot be decoupled into the product of two terms as with the CFNC-SF protocol. In this case, the approach is to directly bound the instantaneous PEP. The probability of decoding $\hat{\boldsymbol{x}}$, namely $\Pr(\hat{\boldsymbol{x}}|\mathbf{h}^{(s)})$, can be bounded as asserted in the following lemma.

Lemma 1. *Let $\mathcal{E}$ denote the set of sources that erroneously decoded at least one symbol in $\boldsymbol{x}$ using* (23)*; i.e., $\mathcal{E}:=\cup_{n=1}^{N}\cup_{k=0}^{K-1}\mathcal{E}_n(k)$. With κ_1,κ_2 denoting positive constants, the conditional probability of decoding $\hat{\boldsymbol{x}}$ given that $\boldsymbol{x}$ was transmitted can be bounded as*

$$\Pr(\hat{\boldsymbol{x}}|\mathbf{h}^{(s)})\leq\kappa_1\exp\left(-\kappa_2\sum_{n\in\mathcal{E}}\min_{m\neq n}\{\gamma_{mn}\}\right). \quad (34)$$

Proof: See Appendix C. ∎

Consider now the term $\Pr(\boldsymbol{x}\to\tilde{\boldsymbol{x}}|\mathbf{h},\mathbf{h}^{(s)},\hat{\boldsymbol{x}})$ in (26), and define matrix $\boldsymbol{\Gamma}_{\hat{x}}$ as

$$\boldsymbol{\Gamma}_{\hat{x}}:=\begin{bmatrix}\mathbf{D}_x(0)\\(\boldsymbol{\Theta}\mathbf{D}_x(1)+\mathbf{D}_\alpha\boldsymbol{\Theta}\hat{\mathbf{X}}(0))\odot\mathbf{I}_N\\\vdots\\(\boldsymbol{\Theta}\mathbf{D}_x(k)+\mathbf{D}_\alpha\boldsymbol{\Theta}\hat{\mathbf{X}}(k-1))\odot\mathbf{I}_N\\\vdots\\(\boldsymbol{\Theta}\mathbf{D}_x(K-1)+\mathbf{D}_\alpha\boldsymbol{\Theta}\hat{\mathbf{X}}(K-2))\odot\mathbf{I}_N\\(\mathbf{D}_\alpha\boldsymbol{\Theta}\hat{\mathbf{X}}(K-1))\odot\mathbf{I}_N\end{bmatrix} \quad (35)$$

where $\hat{\mathbf{X}}(k)$ is defined as

$$\hat{\mathbf{X}}(k) := \begin{bmatrix} 0 & \hat{x}_1^{(2)}(k) & \cdots & \hat{x}_1^{(N)}(k) \\ \hat{x}_2^{(1)}(k) & 0 & \cdots & \hat{x}_2^{(N)}(k) \\ \vdots & \vdots & \ddots & \vdots \\ \hat{x}_N^{(1)}(k) & \hat{x}_N^{(2)}(k) & \cdots & 0 \end{bmatrix}. \quad (36)$$

With these definitions, and using the input-output relationship in (8), the term $\Pr(\boldsymbol{x} \to \tilde{\boldsymbol{x}}|\mathbf{h}, \mathbf{h}^{(s)}, \hat{\boldsymbol{x}})$ is given by [5]

$$\Pr(\boldsymbol{x} \to \tilde{\boldsymbol{x}}|\mathbf{h}, \mathbf{h}^{(s)}, \hat{\boldsymbol{x}}) = Q\left(\frac{\|(\mathbf{\Gamma}_{\hat{x}} - \mathbf{\Gamma}_{\tilde{x}})\mathbf{h}\|^2 - \|(\mathbf{\Gamma}_{\hat{x}} - \mathbf{\Gamma}_{x})\mathbf{h}\|^2}{\sqrt{2\,\|(\mathbf{\Gamma}_{\tilde{x}} - \mathbf{\Gamma}_{x})\mathbf{h}\|^2}}\right) \quad (37)$$

where $\mathbf{\Gamma}_{\tilde{x}}$ is as in (9), after substituting $x_n(k)$ with $\tilde{x}_n(k)$. The terms in (37) can be expressed as

$$\|(\mathbf{\Gamma}_{\hat{x}} - \mathbf{\Gamma}_{\tilde{x}})\mathbf{h}\|^2 = \sum_{n=1}^{N} \tilde{\lambda}_n \gamma_n \quad (38)$$

$$\|(\mathbf{\Gamma}_{\hat{x}} - \mathbf{\Gamma}_{x})\mathbf{h}\|^2 = \sum_{n=1}^{N} \lambda_n \gamma_n \quad (39)$$

where

$$\tilde{\lambda}_n = \sum_{k=0}^{K} \left| \theta_{nn}(x_n(k) - \tilde{x}_n(k)) + \sqrt{\alpha_n} \sum_{\substack{m=1 \\ m \neq n}}^{N} \theta_{nm}(\hat{x}_m^{(n)}(k) - \tilde{x}_m(k)) \right|^2$$

$$\lambda_n = \sum_{k=0}^{K} \left| \sqrt{\alpha_n} \sum_{\substack{m=1 \\ m \neq n}}^{N} \theta_{nm}(\hat{x}_m^{(n)}(k) - x_m(k)) \right|^2$$

are the squared eigenvalues of $\mathbf{\Gamma}_{\hat{x}} - \mathbf{\Gamma}_{\tilde{x}}$ and $\mathbf{\Gamma}_{\hat{x}} - \mathbf{\Gamma}_{x}$, respectively. Clearly, $\lambda_n > 0, \forall n \in \mathcal{E}$ and $\lambda_n = 0, \forall n \in \bar{\mathcal{E}}$. Using this result, the following lemma can be established.

Lemma 2. *Given the CFNC coefficients $\boldsymbol{\theta}_n$ satisfying (2), for any error event $\mathbf{e} := \mathbf{x} - \tilde{\mathbf{x}} = [e_1, e_2, ..., e_N]^T \neq \mathbf{0}$ where $\mathbf{x}, \tilde{\mathbf{x}} \in \mathcal{A}_s^N$, there always exists a (possibly random) variable $\alpha_{n0} > 0$ such that the inequality*

$$\left\| \theta_{nn} e_n + \sqrt{\alpha_n} \sum_{\substack{m=1 \\ m \neq n}}^{N} \theta_{mn} e_m \right\|^2 \geq \alpha_{n0} \alpha_n \left\| \sum_{m=1}^{N} \theta_{mn} e_m \right\|^2 \quad (40)$$

holds with probability 1.

Proof: See Appendix D. ∎

Applying Lemma 2 to (38) and (39), the conditional probability in (37) can be conveniently bounded as asserted in the following lemma.

Lemma 3. *Let $\mathcal{C} = \bar{\mathcal{E}}$ be the set of sources that correctly detected all symbols in $\boldsymbol{x}$ at all phases $k = 0, 1, \ldots, K-1$. With κ_3 and κ_4 denoting positive constants, the conditional error probability in* (37) *can be bounded by*

$$\Pr(\boldsymbol{x} \to \tilde{\boldsymbol{x}}|\mathbf{D}_\alpha, \mathbf{h}, \hat{\boldsymbol{x}}) \leq Q\left(\frac{\kappa_3 \sum_{n\in\mathcal{C}} \alpha_{n0}\alpha_n\gamma_n - \kappa_4 \sum_{n\in\mathcal{E}} \alpha_n\gamma_n}{\sqrt{2\kappa_3 \sum_{n\in\mathcal{C}} \alpha_{n0}\alpha_n\gamma_n + 2\kappa_4 \sum_{n\in\mathcal{E}} \alpha_n\gamma_n}}\right). \quad (41)$$

Proof: See Appendix E. ∎

Combining Lemmas 1 and 3, the PEP in (26) can be further bounded by

$$\Pr(\boldsymbol{x} \to \tilde{\boldsymbol{x}}|\mathbf{h}, \mathbf{h}^{(s)}) \leq \kappa_1 \exp\left(-\kappa_2 \sum_{n\in\mathcal{E}} \min_{m\neq n}\{\gamma_{mn}\}\right) \times Q\left(\frac{\kappa_3 \sum_{n\in\mathcal{C}} \alpha_{n0}\alpha_n\gamma_n - \kappa_4 \sum_{n\in\mathcal{E}} \alpha_n\gamma_n}{\sqrt{2\kappa_3 \sum_{n\in\mathcal{C}} \alpha_{n0}\alpha_n\gamma_n + 2\kappa_4 \sum_{n\in\mathcal{E}} \alpha_n\gamma_n}}\right). \quad (42)$$

This expression is similar to the one encountered in [21, Lemma 2], leading to.

Proposition 3. *(Diversity order of the CFNC-LAF protcol) Given the CFNC coefficients $\boldsymbol{\theta}_n$ satisfying* (2)*, and the link-adaptive power scaling coefficients α_n satisfying* (22)*, the diversity order as defined in* (13) *of the CFNC-LAF protocol is*

$$\min_{\boldsymbol{x}, \tilde{\boldsymbol{x}} \neq \boldsymbol{x}} \left\{ -\lim_{\bar{\gamma}\to\infty} \frac{\log \mathbb{E}_h\left[\Pr(\boldsymbol{x} \to \tilde{\boldsymbol{x}}|\mathbf{h}, \mathbf{h}^{(s)})\right]}{\log \bar{\gamma}} \right\} = N. \quad (43)$$

Proof: See Appendix F. ∎

Both CFNC-LAF and CFNC-SF protocols achieve diversity order equal to the number of sources N. For systems with the same diversity order, comparing relative performance typically relies on their respective coding gains. This will be done through simulations in the following section.

V. Simulations

In the following matrix $\mathbf{\Theta}$ is chosen to have entries $[\mathbf{\Theta}]_{nm} = \theta_{nm} = e^{j\pi(4n-1)(m-1)/(2N)}/\sqrt{N}$ for $N = 2^k$ and $\theta_{nm} = e^{j\pi(6n-1)(m-1)/(3N)}/\sqrt{N}$ for $N = 3 \times 2^k$, $\forall n, m = 1, 2, ..., N$ [26]. Notice that $\mathbf{\Theta}$ is unitary, and so the transmission power is not affected. Unless otherwise stated, $K = 100$, and the Viterbi algorithm is employed to decode $\boldsymbol{x}$ at the destination. Without loss of generality, in all simulations source-destination and source-source links are set to be identical; that is, $\sigma_1^2 = \sigma_2^2 = \cdots = \sigma_N^2$, and $\sigma_{11}^2 = \cdots = \sigma_{1N}^2 = \cdots = \sigma_{NN}^2$. The parameter β in (22) is set to one. For a fair comparison, the transmission power of all schemes has been normalized so that all of them transmit with the same average power. Notice that the specific choice of modulation type or β will not affect the achievable diversity, and so they are not optimized here.

1) Test Case 1 (Diversity performance): Fig. 3 depicts the BER vs. SNR curves of the CFNC-LAF protocol for $N = 2, 3$, and for BPSK and QPSK modulations. The BER of the non-cooperative case is also included for comparison. As seen, diversity of order 2 and 3 can be achieved by the CFNC-LAF protocol. As the number of sources increases, the CFNC suffers performance loss at low SNR. This is because the minimum distance between constellation points is reduced.

2) Test Case 2 (Block transmissions): Here, instead of transmitting symbol-by-symbol, the performance of both CFNC-LAF and CFNC-SF is compared for different block lengths M. For a fair comparison, the CFNC-LAF scheme is modified so that whenever sources correctly demodulate other sources' packages, α_n in (21) is set to 1, otherwise it is as in (22). Fig. 4 plots the BER vs. SNR curves for $N = 2$, BPSK modulation, and $M = 10, 100, 500$. Clearly, diversity of order 2 is achieved by both CFNC-SF and CFNC-LAF

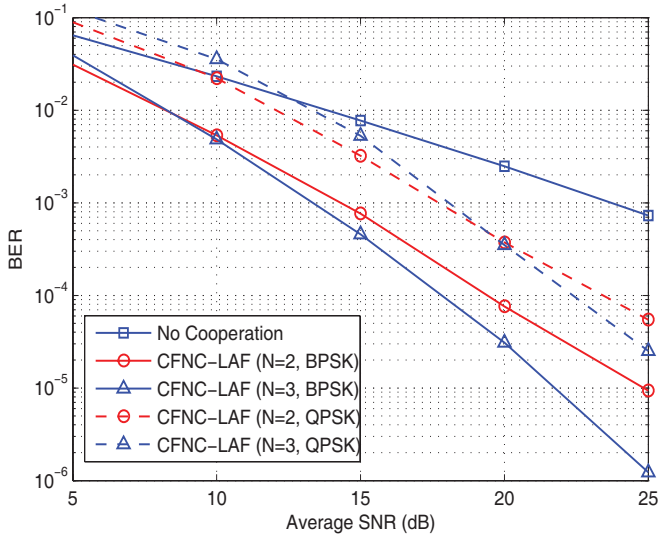

Fig. 3. BER vs. SNR (in dB) curves for CFNC-LAF with $N = 2$ and $N = 3$.

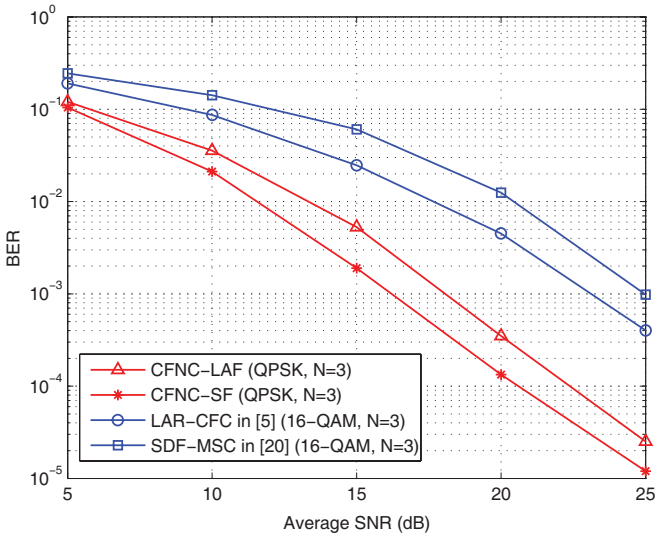

Fig. 5. BER vs. SNR (in dB) curves for CFNC-LAF and distributed space-time methods with $N = 3$ and throughput 2 spspcu.

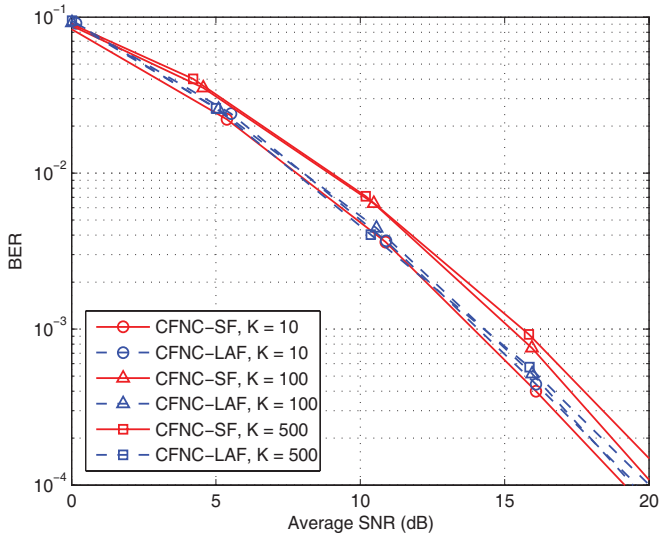

Fig. 4. BER vs. SNR (in dB) curves for the CFNC-LAF and CFNC-SF with $N = 2$, BPSK modulation and message length 10, 100 and 500.

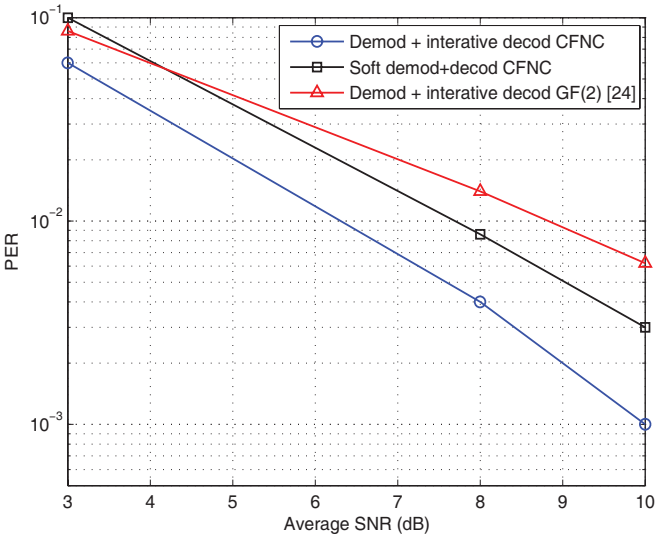

Fig. 6. PER vs. SNR (in dB) curves for the coded CFNC-LAF and bit-level network coding in [24], with $N = 2$ and message length $M = 100$.

regardless of the block length. Since CFNC-LAF forwards packets regardless of the block error outages, the BER curves for different M remain essentially the same; for CFNC-SF, the BER reduces as M increases, since erroneous packets are discarded at intermediate stages, even when only a few bits are present.

3) Test Case 3 (Comparisons with distributed space-time coding): Fig. 5 compares the performance of [5], [20] with that of the CFNC-SF and CFNC-LAF protocols for $N = 3$ and $M = 1$. Due to the fact that the achievable throughput of CFNC-based schemes nearly reaches $1/N$ spspcu, which is twice as high as that of the schemes in [5], [20], QPSK modulation is used for the non-cooperative and CFNC cases, whereas 16-QAM is used for the protocols in [5], [20]. As expected, all cooperative schemes in Fig. 5 achieve diversity order 3, but the CFNC protocols achieve more than 5 dB coding gain advantage. The CFNC-SF requires extra overhead to accommodate CRC codes (same as [20]); whereas the CFNC-LAF requires extra training pilots for each link and feedback of the average SNR (same as [5]).

4) Test Case 4 (Coded transmissions): Here, coded transmissions are considered and compared with the network coding protocol in [24]. Convolutional codes of rate $\frac{1}{3}$ with generator polynomials $[1, \frac{13}{15}, \frac{17}{15}]_8$ for local information bits and $[\frac{02}{15}, \frac{07}{15}, 1]_8$ for the relayed ones are used. Soft iterative decoding is employed at the destination. For the scheme in this paper, two different approaches are considered: i) soft demodulation and decoding; and ii) soft demodulation and iterative decoding along the lines of [24]. For simplicity, in all protocols sources incur no detection error when decoding packets from other sources (and thus the CFNC-SF and CFNC-LAF protocols are the same). The number of information bits per packet is 100; thus, the corresponding coded packet length is 300. As shown in Fig. 6, both CFNC-based protocols entail coding gain advantage over the network-coding-based scheme in [24]. This is because the CFNC scheme exploits

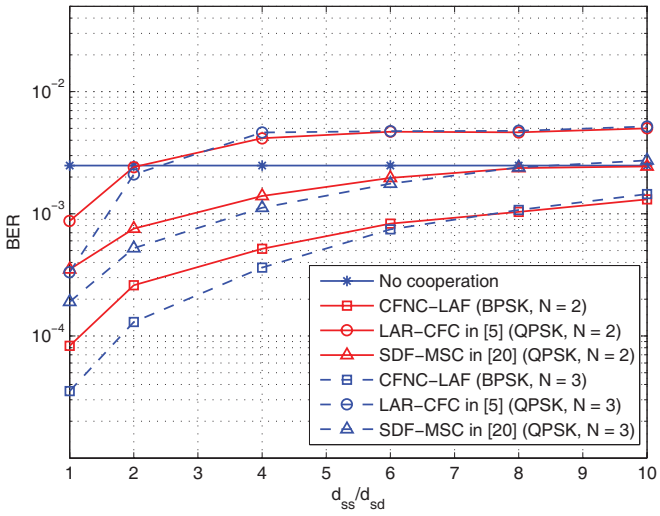

Fig. 7. BER vs. different source-destination or source-source distances for CFNC-LAF with $N = 2, 3$ and average SNR=20dB .

more degrees of freedom by coding information in both complex field and GF(2) rather than GF(2) alone as in [24]. Compared to superposition coding as in [17], notice that [24] already provides performance comparisons with [17]. Since the developed scheme outperforms [24], it also outperforms [17].

5) Test Case 5 (Effect of inter-source errors): Here, the BER of the CFNC-LAF is tested for various source-source and source-destination distances, denoted by d_{ss} and d_{sd}, respectively. These distances are taken inversely proportional to the average channel gain; i.e., $d_{sd} \propto \sigma_{sd}^{-2}$ and $d_{ss} \propto \sigma_{ss}^{-2}$. Fig. 7 depicts the BER performance when $N = 2, 3$. The non-cooperative case is also included for comparison. When sources are far apart from each other (d_{ss} is relatively large), the BER performance of CFNC-LAF approaches that of the non-cooperative case. However, when sources are close to each other (d_{ss} is relatively small), the CFNC-LAF outperforms its non-cooperative counterpart as well as the schemes in [5], [20]. These observations imply that in practice sources that are close are encouraged to transmit cooperatively.

VI. Conclusions

Robust and high-throughput CFNC protocols were developed using symbol-level physical-layer network coding operations, and selective- or link-adaptive-forwarding. The throughput of the novel protocol is approximately $1/N$ symbols per source per channel use (spspcu), and achieves spatial diversity N for N cooperating sources. The CFNC-SF achieves this by invoking error-detection codes; whereas the CFNC-LAF requires extra training pilots per link and feedback of the average SNR coefficient, which varies at a slow time scale. Fading coefficients h_n are not needed at the sources; thus, neither CFNC-SF nor CFNC-LAF requires instantaneous feedback from the destination. Simulated tests demonstrated full diversity and coding gain advantage compared to distributed space-time coding, and bit-level network coding alternatives.

Appendix A
Proof of Proposition 1

Proving that $\text{rank}(\mathbf{\Gamma}_x - \mathbf{\Gamma}_{\tilde{x}}) = N$ is equivalent to showing that there exists a Phase-k such that

$$\text{rank}\left(\begin{bmatrix} (\mathbf{\Theta}\mathbf{D}_x(k)+\mathbf{\Theta}\mathbf{X}(k-1))\odot\mathbf{I}_N \\ (\mathbf{\Theta}\mathbf{D}_x(k+1)+\mathbf{\Theta}\mathbf{X}(k))\odot\mathbf{I}_N \end{bmatrix} - \begin{bmatrix} (\mathbf{\Theta}\mathbf{D}_{\tilde{x}}(k)+\mathbf{\Theta}\tilde{\mathbf{X}}(k-1))\odot\mathbf{I}_N \\ (\mathbf{\Theta}\mathbf{D}_{\tilde{x}}(k+1)+\mathbf{\Theta}\tilde{\mathbf{X}}(k))\odot\mathbf{I}_N \end{bmatrix} \right) = N \quad (44)$$

where $\mathbf{X}(-1) := \mathbf{0}_{N\times N}$ and $\mathbf{D}_x(K+1) := \mathbf{0}_{N\times N}$. Equation (44) can be written as

$$\text{rank}\begin{bmatrix} \text{diag}(\mathbf{D}_\theta\mathbf{e}(k) + \tilde{\mathbf{\Theta}}\mathbf{e}(k-1)) \\ \text{diag}(\mathbf{D}_\theta\mathbf{e}(k+1) + \tilde{\mathbf{\Theta}}\mathbf{e}(k)) \end{bmatrix} = N \quad (45)$$

where $\mathbf{e}(k) := \mathbf{x}(k) - \tilde{\mathbf{x}}(k)$, $\mathbf{x}(k)$: $= [x_1(k), \ldots, x_N(k)]^T$, $\tilde{\mathbf{x}}(k) := [\tilde{x}_1(k), \ldots, \tilde{x}_N(k)]^T$; and $\mathbf{D}_\theta$, $\tilde{\mathbf{\Theta}}$ are matrices containing the diagonal and off-diagonal elements of $\mathbf{\Theta}$. The m-th diagonal entry of $\text{diag}(\mathbf{D}_\theta\mathbf{e}(k) + \tilde{\mathbf{\Theta}}\mathbf{e}(k-1))$ (the upper diagonal matrix in (45)) can be written as $\boldsymbol{\theta}_m^T\tilde{\mathbf{e}}(k)$, where $\boldsymbol{\theta}_m$ is the m-th row of $\mathbf{\Theta}$, and $[\tilde{\mathbf{e}}(k)]_n = [\mathbf{e}(k)]_n$ if $n = m$, while $[\tilde{\mathbf{e}}(k)]_n = [\mathbf{e}(k-1)]_n$, otherwise. Likewise, the m-th diagonal entry of $\text{diag}(\mathbf{D}_\theta\mathbf{e}(k+1)+\tilde{\mathbf{\Theta}}\mathbf{e}(k))$ (the lower diagonal matrix in (45)) can be written as $\boldsymbol{\theta}_m^T\tilde{\mathbf{e}}(k+1)$. Supposing $\mathbf{e}(k) \neq \mathbf{0}$ (since $\boldsymbol{x} \neq \tilde{\boldsymbol{x}}$, so that a phase k in which $\mathbf{e}(k) \neq \mathbf{0}$ can always be found), if $\mathbf{e}(k)$ is non-zero at its m-th entry, $\tilde{\mathbf{e}}(k)$ is non-zero at its m-th entry too; otherwise, if $\mathbf{e}(k)$ is zero at its m-th entry, $\tilde{\mathbf{e}}(k+1)$ will be non-zero because at least one entry $n \neq m$ is non-zero. Thus, in order to achieve full rank N, it is sufficient to design $\mathbf{\Theta}$ so that $\boldsymbol{\theta}_m^T\tilde{\mathbf{e}}(k) \neq 0$ for $\tilde{\mathbf{e}}(k) \neq \mathbf{0}$ and $\boldsymbol{\theta}_m^T\tilde{\mathbf{e}}(k+1) \neq 0$ for $\tilde{\mathbf{e}}(k+1) \neq \mathbf{0}$,$\forall m = 1, ..., N$, which coincides with condition (2).

Appendix B
Proof of Proposition 2

First, it will be shown that the diversity order of $\mathbb{E}_{\mathbf{h}^{(s)}}[\Pr(\boldsymbol{x} \to \tilde{\boldsymbol{x}}|\mathbf{h}, \hat{\boldsymbol{x}})]$ is at least $N - |\mathcal{E}|$. To this end, one can prove that for any k

$$\text{rank}\left(\begin{bmatrix} (\mathbf{\Theta}\mathbf{D}_x(k)+\mathbf{\Theta}\mathbf{X}_\mathcal{D}(k-1))\odot\mathbf{I}_N \\ (\mathbf{\Theta}\mathbf{D}_x(k+1)+\mathbf{\Theta}\mathbf{X}_\mathcal{D}(k))\odot\mathbf{I}_N \end{bmatrix} - \begin{bmatrix} (\mathbf{\Theta}\mathbf{D}_{\tilde{x}}(k)+\mathbf{\Theta}\tilde{\mathbf{X}}_\mathcal{D}(k-1))\odot\mathbf{I}_N \\ (\mathbf{\Theta}\mathbf{D}_{\tilde{x}}(k+1)+\mathbf{\Theta}\tilde{\mathbf{X}}_\mathcal{D}(k))\odot\mathbf{I}_N \end{bmatrix} \right) \geq N - |\cup_{m=1}^N \mathcal{E}_m(k)| \quad (46)$$

where $\mathbf{X}_\mathcal{D}(k)$ ($\tilde{\mathbf{X}}_\mathcal{D}(k)$) is defined as $\mathbf{X}(k)$ ($\tilde{\mathbf{X}}(k)$), after setting $[\mathbf{X}(k)]_{m,n} = 0$ ($[\tilde{\mathbf{X}}(k)]_{m,n} = 0$) whenever $m \notin \mathcal{D}_n(k)$. Following the same steps as in Appendix A, it can be shown that the error event $m \notin \mathcal{D}_n(k)$ decreases the rank of (46) by at most one $\forall m$. Given the relationship between sets $\mathcal{D}_n(k)$ and $\mathcal{E}_m(k)$ in (29), this is equivalent to asserting that whenever $n \notin \mathcal{E}_m(k)$ the rank of (46) is reduced by at most one. Considering all error events, this implies that the rank of (46) is reduced by at most $|\cup_{m=1}^N \mathcal{E}_m(k)|$, and the rank of $\mathbf{\Gamma}_x(\mathcal{D}) - \mathbf{\Gamma}_{\tilde{x}}(\mathcal{D})$ is reduced by at most $|\cup_{k=1}^K \cup_{m=1}^N \mathcal{E}_m(k)| = |\mathcal{E}|$. Substituting

this result into (32) and using (30), the average PEP expression in (27) now yields

$$\mathbb{E}_{\mathbf{h},\mathbf{h}^{(s)}}\Big[\Pr(\boldsymbol{x}\to\tilde{\boldsymbol{x}}|\mathbf{h},\mathbf{h}^{(s)})\Big]\leq\sum_{\forall\mathcal{E}}(\beta'\bar{\gamma})^{-|\mathcal{E}|}(\beta''\bar{\gamma})^{-N+|\mathcal{E}|}=(\beta'''\bar{\gamma})^{-N} \tag{47}$$

where β''' is a positive constant. Thus, the diversity order is independent of the inter-source error events and equals the number of sources N.

Appendix C
Proof of Lemma 1

The symbol error probability for source U_n when estimating $x_m(k)$ at phase $k>1$ depends on the symbols $\hat{x}_p^{(n)}(k-1)$ detected in the previous phase [cf. (23)]. Let $\mathcal{G}_{nm}(k):=\{p|\hat{x}_p^{(n)}(k-1)\neq\hat{x}_p^{(m)}(k-1),p=1,\ldots,N\}$ denote the set of symbols for which sources U_n and U_m have different estimates of. The symbol error probability for source U_n when estimating $x_m(k)$ can be written as

$$\begin{aligned}p_m^{(n)}(k)&=\Pr\{x_m^{(n)}(k)\neq x_m(k)\}\\&=\Pr\{x_m^{(n)}(k)\neq x_m(k),\mathcal{G}_{mn}(k)\neq\emptyset\}\\&\quad+\Pr\{x_m^{(n)}(k)\neq x_m(k),\mathcal{G}_{mn}(k)=\emptyset\}.\end{aligned} \tag{48}$$

According to the detector in (5), and assuming PSK or QAM modulations, the second term on the r.h.s. of (48) is given by

$$\begin{aligned}\Pr\{x_m^{(n)}(k)\neq x_m(k),\mathcal{G}_{mn}(k)=\emptyset\}&=Q\left(\sqrt{c_0\left|h_{mn}\right|^2\bar{\gamma}}\right)\\&\leq\exp\left(-c_0\gamma_{mn}\right)\end{aligned} \tag{49}$$

where c_0 is a positive constant that depends on the type of modulation [19]. The first term in (48) can be bounded as follows

$$\begin{aligned}&\Pr\{x_m^{(n)}(k)\neq x_m(k),\mathcal{G}_{nm}(k)\neq\emptyset\}\\&=Q\left(\sqrt{c_0\left|h_{mn}\right|^2\bar{\gamma}}\big(1-\sqrt{\textstyle\sum_{p\in\mathcal{G}_{mn}(k)}c_p\alpha_p}\big)\right)\\&=Q\left(\sqrt{c_0\left|h_{mn}\right|^2\bar{\gamma}}\big(1-\sqrt{\textstyle\sum_{p\in\mathcal{G}_{mn}(k)}c_p\beta\min\{1,\min_{l'\neq p}\frac{\gamma_{pp'}}{\bar{\gamma}}\}}\big)\right)\\&\leq Q\left(\sqrt{c_0\left|h_{mn}\right|^2\bar{\gamma}}\big(1-\sqrt{N\beta\max_{p\in\mathcal{G}_{mn}(k)}\{c_p\}}\big)\right)\\&\leq\exp\left(-c_0'\gamma_{mn}\right)\end{aligned} \tag{50}$$

where $c_0'\leq c_0\left(1-\sqrt{N\beta\max_p\{c_p\}}\right)$ is a positive constant for any β such that $0\leq N\beta\max_p\{c_p\}<1$. Combining these two results, $p_m^{(n)}(k)$ can be bounded as $\exp\left(-\kappa'\gamma_{mn}\right)$ with $\kappa'>0$, and thus $\Pr(\boldsymbol{x}\to\hat{\boldsymbol{x}}|\mathbf{h}^{(s)})$ can be bounded as

$$\begin{aligned}\Pr(\boldsymbol{x}\to\hat{\boldsymbol{x}}|\mathbf{h}^{(s)})&=\prod_{n\in\mathcal{E}}\Big[1-\prod_{k=0}^{K-1}\prod_{\substack{m=1\\m\neq n}}^{N}(1-p_m^{(n)}(k))\Big]\\&\leq\prod_{n\in\mathcal{E}}(N-1)K\exp\left(-\kappa'\min_{m\neq n}\{\gamma_{mn}\}\right)\\&\leq\kappa_1\exp\left(-\kappa_2\sum_{n\in\mathcal{E}}\min_{m\neq n}\{\gamma_{mn}\}\right)\end{aligned} \tag{51}$$

where $\kappa_1:=((N-1)K)^{|\mathcal{E}|}$, and $\kappa_2:=\kappa'$.

Appendix D
Proof of Lemma 2

Clearly this lemma holds for $\alpha_n=1$. Since $\Pr(\alpha=0)=0$, only the case $0<\alpha_n<1$ will be considered in the following. Let $v_1:=\theta_{nn}e_n$, $v_2:=\sum_{m=1,m\neq n}^{N}\theta_{nm}e_m$ and denote α_n by α for all $n=1,2,...,N$. Consider the angles ϕ_0, ϕ_1, ϕ_2 and ϕ_3 defined as shown in Fig. 8. The proof of this lemma can be split into the following cases:

- $\pi/2\leq\phi_1<\pi$ (Fig. 8(a)): In this case it holds that $\phi_0>\phi_1$ and thus $\phi_0>\pi/2$, which means
$$|v_1+\sqrt{\alpha}v_2|^2>\alpha|v_1+v_2|^2 \tag{52}$$
and the lemma holds for any $\alpha_0\in(0,1]$.
- $0<\phi_2\leq\pi/2$ (Fig. 8(b)): In this case since (52) still holds for $\phi_0=\pi-\phi_2>\pi/2$ the lemma holds for any $\alpha_0\in(0,1]$.
- $0<\phi_1\leq\pi/2$ and $\pi/2\leq\phi_2<\pi$ (Fig. 8(c)): In this case it holds that $\phi_0=\pi-\phi_2<\pi/2$. For $\phi_3<\phi_0$, (52) still holds. But because the angle ϕ_3 decreases with ϕ_2 and α, it follows that $\phi_3<\phi_0$ holds whenever $\alpha>\alpha_e$ where
$$\alpha_e=\left(\frac{|v_1|}{2|v_2|\cos\phi_1-|v_1|}\right)^2 \tag{53}$$
which comes from the equality $|v_1+\sqrt{\alpha_e}v_2|^2=\alpha_e|v_1+v_2|^2$. Note that here $\alpha_e<1$ is guaranteed because $|v_2|\cos\phi_1>|v_1|$ since $\phi_2>\pi/2$. This implies that $|v_1+\sqrt{\alpha}v_2|^2<\alpha|v_1+v_2|^2$ for $\alpha>\alpha_e$. Fortunately, it can be found from Fig. 8(c) that the following inequality holds $|v_1+\sqrt{\alpha}v_2|^2\geq\alpha_e\alpha|v_1+v_2|^2$. Therefore, α_0 can be set to any positive value less than α_e to satisfy (40); e.g., $\alpha_0=\left(\frac{|v_1|}{2|v_2|}\right)^2$.

Similar arguments can be made for the extreme cases $\phi_1=0$ and $\phi_1=\pi$.

Appendix E
Proof of Lemma 3

From (38) and (39), it holds that

$$\begin{aligned}\|(\mathbf{\Gamma}_{\hat{x}}-\mathbf{\Gamma}_x)\mathbf{h}\|^2&\leq\|(\mathbf{\Gamma}_{\hat{x}}-\mathbf{\Gamma}_{\tilde{x}})\mathbf{h}\|^2+\|(\mathbf{\Gamma}_{\hat{x}}-\mathbf{\Gamma}_x)\mathbf{h}\|^2\\&=\sum_{n=1}^{N}\tilde{\lambda}_n\left|h_n\right|^2+\sum_{n=1}^{N}\lambda_n\left|h_n\right|^2.\end{aligned} \tag{54}$$

According to Lemma 2, it follows that

$$\begin{aligned}&\Pr(\boldsymbol{x}\to\tilde{\boldsymbol{x}}|\mathbf{h},\mathbf{h}^{(s)},\hat{\boldsymbol{x}})\\&\quad\leq Q\left(\frac{\sum_{n=1}^{N}\tilde{\lambda}_n\left|h_n\right|^2-\sum_{n=1}^{N}\lambda_n\left|h_n\right|^2}{\sqrt{2\sum_{n=1}^{N}\tilde{\lambda}_n\left|h_n\right|^2+2\sum_{n=1}^{N}\lambda_n\left|h_n\right|^2}}\right).\end{aligned} \tag{55}$$

Using Lemma 2, and the fact that $\lambda_n>0$ for any $n\in\mathcal{E}$ and $\lambda_n=0$ for any $n\in\bar{\mathcal{E}}$, the expression $\|(\mathbf{\Gamma}_{\hat{x}}-\mathbf{\Gamma}_{\tilde{x}})\mathbf{h}\|^2$ can be bounded by

$$\|(\mathbf{\Gamma}_{\hat{x}}-\mathbf{\Gamma}_{\tilde{x}})\mathbf{h}\|^2\geq\sum_{n\in\mathcal{C}}\tilde{\lambda}_n\left|h_n\right|^2\geq\kappa_3\sum_{n\in\mathcal{C}}\alpha_{n0}\alpha_n\bar{\gamma}\left|h_n\right|^2 \tag{56}$$

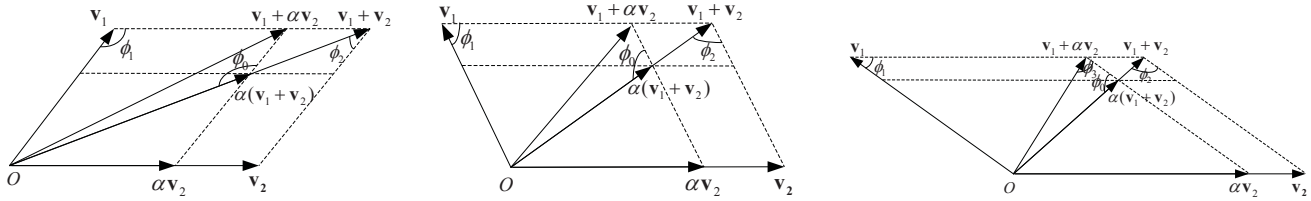

(a) $\frac{\pi}{2} < \phi_1 < \pi$ (b) $0 < \phi_2 < \frac{\pi}{2}$ (c) $0 < \phi_1 < \frac{\pi}{2}$ and $\frac{\pi}{2} < \phi_2 < \pi$

Fig. 8. The proof of Lemma 2

where $\Pr\{\alpha_{n0} > 0\} = 1$ and

$$\kappa_3 = \min_{n\in\mathcal{C}}\Big\{ \sum\nolimits_{k=0}^{K} \rho_n(k)\Big|\theta_{nn}(x_n(k) - \tilde{x}_n(k)) + \sum_{\substack{m=1\\ m\neq n}}^{N} \theta_{nm}(\hat{x}_m^{(n)}(k) - \tilde{x}_m(k))\Big|^2\Big\}.$$

Likewise, $\|(\mathbf{\Gamma}_{\hat{x}} - \mathbf{\Gamma}_x)\mathbf{h}\|^2$ can be bounded by

$$\|(\mathbf{\Gamma}_{\hat{x}} - \mathbf{\Gamma}_x)\mathbf{h}\|^2 = \sum_{n\in\mathcal{E}} \lambda_n |h_n|^2 \leq \kappa_4 \sum_{n\in\mathcal{E}} \alpha_n \bar{\gamma} |h_n|^2 \quad (57)$$

for some constant κ_4. Substituting (56) and (57) into (55) and setting $\kappa_5 = \sqrt{2}$ yields (41).

APPENDIX F
PROOF OF PROPOSITION 3

It follows from (42) that

$$\Pr(\boldsymbol{x} \to \tilde{\boldsymbol{x}}|\mathbf{h}, \mathbf{h}^{(s)}) \leq \sum_{\forall \tilde{\boldsymbol{x}}} \kappa_1 \exp\Big(-\kappa_2 \sum_{n\in\mathcal{E}} \min_{m\neq n}\{\gamma_{mn}\}\Big)$$
$$\times Q\left(\frac{\kappa_3 \min_{n\in\mathcal{C}}\{\alpha_{n0}\alpha_n\} \sum_{n\in\mathcal{C}} \gamma_{dn} - \kappa_4 \max_{n\in\mathcal{E}} |h_n|^2 \sum_{n\in\mathcal{E}} \min_{m\neq n} \gamma_{mn}}{\kappa_5 \sqrt{\kappa_3 \min_{n\in\mathcal{C}}\{\alpha_{n0}\alpha_n\} \sum_{n\in\mathcal{C}} \gamma_{dn} + \kappa_4 \max_{n\in\mathcal{E}} |h_n|^2 \sum_{n\in\mathcal{E}} \min_{m\neq n} \gamma_{mn}}}\right)$$
$$= \sum_{\forall \tilde{\boldsymbol{x}}} \exp(-\eta'_e \gamma_e) Q\left(\frac{\eta_c\gamma_c - \eta_e\gamma_e}{\kappa_5\sqrt{\eta_c\gamma_c + \eta_e\gamma_e}}\right) \quad (58)$$

where $\gamma_{dn} := |h_n|^2\bar{\gamma}$, $\eta_{e'} := \kappa_2$, $\gamma_c := \sum_{n\in\mathcal{C}} \gamma_{dn}$, $\eta_c := \kappa_3 \min_{n\in\mathcal{C}}\{\alpha_{n0}\alpha_n\}$, $\gamma_e := \sum_{n\in\mathcal{E}} \min_{m\neq n} \gamma_{mn}$ and $\eta_e := \kappa_4 \max_{n\in\mathcal{E}} |h_n|^2$. As seen, γ_c and γ_e are independent and follow a Gamma distribution; thus, they comply with [5, Lemma 2], which is all required to deduce the full diversity of order N.

ACKNOWLEDGEMENT

G. Li would like to thank G. B. Giannakis for the opportunity to visit SPiNCOM at the University of Minnesota during 2009-2010. A. Cano would like to thank A. I. Pérez-Neira for the opportunity to visit the Technical University of Catalonia during summer 2008.

REFERENCES

[1] R. Ahlswede, N. Cai, S.-Y. R. Li, and R. W. Yeung, "Network information flow," *IEEE Trans. Inf. Theory*, vol. 46, no. 4, pp. 1204–1216, July 2000.

[2] K. Azarian, H. Gamal, and P. Schniter, "On the achievable diversity-multiplexing tradeoff in half-duplex cooperative channels," *IEEE Trans. Inf. Theory*, vol. 51, no. 12, pp. 4152-4172, Dec. 2005.

[3] E. Beres and R. Adve, "Selection cooperation in multi-source cooperative networks," *IEEE Trans. Wireless Commun.*, vol. 7, no. 1, pp. 118-127, Jan. 2008

[4] A. Cano, J. Gómez-Vilardebó, A. I. Pérez-Neira, and G. B. Giannakis, "High-rate distributed multi-source cooperation using complex-field coding," in *Proc. Intl. Conf. on Acoustics, Speech and Signal Process.*, Apr. 2009, pp. 2633–2636.

[5] A. Cano, T. Wang, A. Ribeiro, and G. B. Giannakis, "Link-adaptive distributed coding for multisource cooperation," *EURASIP J. Adv. Signal Process.*, vol. 2008, no. 38, pp. 1-12, Jan. 2008.

[6] Y. Chen, S. Kishore, and J. Li, "Wireless diversity through network coding," in *Proc. of Wireless Commun. & Netw. Conf.*, Apr. 2006, pp. 1681–1686.

[7] G. Choi, W. Zhang, and X. Ma, "Diversity-enabled power profile design for relay networks," in *Proc. Military Commun.*, Nov. 2008, pp. 1–7.

[8] P. A. Chou and Y. Wu, "Network coding for the Internet and wireless networks," *IEEE Signal Process. Mag.*, vol. 24, no. 5, pp. 77–85, Sep. 2007.

[9] T. Cover and C. Leung, "An achievable rate region for the multiple-access channel with feedback," *IEEE Trans. Inf. Theory*, vol. 27, no. 3, pp. 292–298, May 1981.

[10] Z. Ding, T. Ratnarajah, and C. Cowan, "On the diversity-multiplexing tradeoff for wireless cooperative multiple access systems," *IEEE Trans. Signal Process.*, vol. 55, no. 9, pp. 4627–4638, Sep. 2007.

[11] Z. Ding, Y. Gong, T. Ratnarajah, and C. Cowan, "On the performance of opportunistic cooperative wireless networks," *IEEE Trans. Commun.*, vol. 56, no. 8, pp. 1236-1240, Aug. 2008.

[12] Z. Han, X. Zhang, and H. V. Poor, "High performance cooperative transmission protocols based on multiuser detection and network coding," *IEEE Trans. Wireless Commun.*, vol. 8, no. 5, pp. 2352–2361, May 2009.

[13] S. Katti, H. Rahul, W. Hu, D. Katabi, M. Medard, and J. Crowcroft, "XORs in the air: practical wireless network coding," *IEEE/ACM Trans. Networking*, vol. 16, no. 3, pp. 497–510, June 2008.

[14] T. Koike-Akino, P. Popovski, and V. Tarokh, "Optimized constellations for two-way wireless relaying with physical network coding," *IEEE J. Sel. Areas Commun.*, vol. 27, no. 5, pp. 773–787, June 2009.

[15] J. N. Laneman, D. N. C. Tse, and G. W. Wornell, "Cooperative diversity in wireless networks: efficient protocols and outage behavior," *IEEE Trans. Inf. Theory*, vol. 50, no. 12, pp. 3062–3080, Dec. 2004.

[16] J. N. Laneman and G. W. Wornell, "Distributed space-time-coded protocols for exploiting cooperative diversity in wireless networks," *IEEE Trans. Inf. Theory*, vol. 49, no. 10, pp. 2415–2425, Oct. 2003.

[17] E. G. Larsson and B. R. Vojcic, "Cooperative transmit diversity based on superposition modulation," *IEEE Commun. Lett.*, vol. 9, no. 9, pp. 778-780, Sep. 2005.

[18] A. Nosratinia, T. E. Hunter, and A. Hedayat, "Cooperative communication in wireless networks," *IEEE Commun. Mag.*, vol. 42, no. 10, pp. 74–80, Oct. 2004.

[19] J. G. Proakis, *Digital Communications*, 4th edition. McGraw-Hill, 2001.

[20] A. Ribeiro, R. Wang, and G. B. Giannakis, "Multi-source cooperation with full-diversity spectral-efficiency and controllable-complexity," *IEEE J. Sel. Areas Commun.*, vol. 25, no. 2, pp. 415–425, Feb. 2007.

[21] T. Wang and G. B. Giannakis, "Complex field network coding for multiuser cooperative communications," *IEEE J. Sel. Areas Commun.*, vol. 26, no. 3, pp. 561–571, Apr. 2008.

[22] T. Wang, G. B. Giannakis, and R. Wang, "Smart regenerative relays for link-adaptive cooperation," *IEEE Trans. Commun.*, vol. 56, no. 11, pp. 1950-1960, Nov. 2008

[23] L. Xiao, D. J. Costello, and T. E. Fuja, "Network coded cooperative diversity with multiple sources," in *Proc. Global Telecommun. Conf.*, Nov. 2009, pp. 1–5.

[24] L. Xiao, T. E. Fuja, J. Kliewer, and D. J. Costello, "A network coding approach to cooperative diversity," *IEEE Trans. Inf. Theory*, vol. 53, no. 10, pp. 3714–3722, Oct. 2007.
[25] M. Xiao and M. Skoglund, "M-user cooperative wireless communications based on nonbinary network codes," *IEEE Inf. Theory Workshop on Netw. & Inf. Theory*, June 2009, pp. 316–320.
[26] Y. Xin, Z. Wang, and G. B. Giannakis, "Space-time diversity systems based on linear constellation precoding," *IEEE Trans. Wireless Commun.*, vol. 2, no. 2, pp. 294-309, Mar. 2003.
[27] G. Yue, X. Wang, Z. Yang, and A. Host-Madsen, "Coding schemes for user cooperation in low-power regimes," *IEEE Trans. Signal Process.*, vol. 56, no. 5, pp. 2035–2049, May 2008.
[28] J. Zhang, K. B. Letaief, and P. Fan, "A distributed product coding approach for robust network coding," in *Proc. Intl. Conf. on Commun.*, May 2008, pp. 176–180.
[29] R. Zhang and L. Hanzo, "Coding schemes for energy efficient multi-source cooperation aided uplink transmission," *IEEE Signal Process. Lett.*, vol. 16, no. 5, pp. 438–441, May 2009.
[30] S. Zhang, S.-C. Liew, and P. P. Lam, "Hot topic: physical-layer network coding," in *Proc. Intl. Conf. Mobile Computing and Netw.,* Sep. 2006, pp. 358–365.

Guobing Li (S'07) received his B.S. and M.Sc. degrees in Electrical Engineering from Xidian University, Xi'an, China in 2001 and 2004, respectively. He is currently working towards the Ph.D. degree with the School of Electronic and Information Engineering, Xi'an Jiaotong University, Xi'an, China. During 2009-2010 he was a visiting student at the Department of Electrical and Computer Engineering, University of Minnesota. His research interests include cooperative communications, network coding and spectrum sensing in cognitive radio systems.

Alfonso Cano received the Telecommunication Engineering and Ph.D. degrees with honors from the Universidad Carlos III de Madrid, Madrid, Spain, in 2002 and 2006, respectively. During 2003-2006, he was with the Dept. of Signal Theory and Communications, Universidad Rey Juan Carlos, Madrid, Spain. Since 2007 he is with the ECE Department at the Univ. of Minnesota, MN USA, where he is a Post-doctoral researcher. His research interests lie in the areas of signal processing and communications.

Jesús Gómez-Vilardebó received his M. Sc. and Ph.D. degrees in Telecommunication Engineering from the Universitat Politècnica de Catalunya (UPC) in October 2003 and July 2009, respectively. In September 2005, he was granted by the Centre Tecnològic de Telecomunicacions de Catalunya (CTTC) to obtain the Ph. D. on Signal Theory and Communications at the UPC. He is now with the CTTC holding a Research Associate position. His primary research interests include information-theory and cooperative multi-hop wireless communication.

Georgios B. Giannakis (Fellow'97) received his Diploma in Electrical Engr. from the Ntl. Tech. Univ. of Athens, Greece, 1981. From 1982 to 1986 he was with the Univ. of Southern California (USC), where he received his MSc. in Electrical Engineering, 1983, MSc. in Mathematics, 1986, and Ph.D. in Electrical Engr., 1986. Since 1999 he has been a professor with the Univ. of Minnesota, where he now holds an ADC Chair in Wireless Telecommunications in the ECE Department, and serves as director of the Digital Technology Center.

His general interests span the areas of communications, networking and statistical signal processing - subjects on which he has published more than 300 journal papers, 500 conference papers, two edited books and two research monographs. Current research focuses on compressive sensing, cognitive radios, network coding, cross-layer designs, mobile ad hoc networks, wireless sensor and social networks. He is the (co-)inventor of twenty patents issued, and the (co-)recipient of seven paper awards from the IEEE Signal Processing (SP) and Communications Societies, including the G. Marconi Prize Paper Award in Wireless Communications. He also received Technical Achievement Awards from the SP Society (2000), from EURASIP (2005), a Young Faculty Teaching Award, and the G. W. Taylor Award for Distinguished Research from the University of Minnesota. He is a Fellow of EURASIP, and has served the IEEE in a number of posts, including that of a Distinguished Lecturer for the IEEE-SP Society.

Ana I. Pérez-Neira (S'92, M'95, SM'02) is full professor at UPC (Technical University of Catalonia) in the Signal Theory and Communication department. Her research field is signal processing applied to wireless communications (both mobile and satellite). She has been the leader of 18 projects (seven international and 11 national). She is author of 25 journal papers (SCI indexed) and more than 150 conference papers (18 invited). She is co-author of four books and three patents. She has been in the board of directors of ETSETB (Telecom Barcelona) from 2000-03 and currently she is in the board of directors of CTTC (Centre Tecnologic de Telecomnicacions de Catalonia). She is member of Eurasip Adcom (European Signal Processing Association) and of IEEE SPTM (Signal Processing Theory and Methods). She has been visiting professor at KTH (Royal Institute Stockholm) during six months and at Shandong University (China) during one month. She is an editor of JASP (*Journal of Advances in Signal Processing* of Hindawi) and a reviewer of various journals and organizations. She has chaired two international conferences, IWCLD09 and EUSIPCO 2011, and participated in the organization of other two (ESA conference'96, SAM'04). Currently she is Vice Chancellor at UPC.